

---

# A SKY SURVEY OF ULTRAVIOLET SOURCES OBSERVED THROUGH ASTROSAT'S UVIT: A POINT SOURCE CATALOG

---

**Swagat Bordoloi, Rupjyoti Gogoi**

Department of Physics, Tezpur University, Napaam, 784028, Assam, India

**P. Shalima**

Manipal Centre for Natural Sciences, Manipal Academy of Higher Education, Manipal, 576104, Karnataka, India

**Jayant Murthy**

Indian Institute of Astrophysics, Bengaluru, 560034, Karnataka, India

## ABSTRACT

The Ultra Violet Imaging Telescope (UVIT) onboard India's first dedicated multiwavelength satellite *AstroSat* observed a significant fraction of the sky in the ultraviolet with a spatial resolution of  $1.4''$ . We present a catalog of the point sources observed by UVIT in the far ultraviolet (FUV; 1300-1800 Å) and near ultraviolet (NUV; 2000-3000 Å). We carried out astrometry and photometry of 428 field pointings in the FUV and 54 field pointings in the NUV band, observed in 5 filter bands in each channel respectively, covering an area of about 63 square degrees. The final catalog contains about 102,773 sources. The limiting magnitude(AB) of the F148W band filter, that has the largest number of detections is  $\sim 21.3$ . For the NUV channel, we find the limiting magnitude at around  $\sim 23$ . We describe the final catalog and present the results of the statistical analysis.

## 1 Introduction

The Indian Space Research Organisation (ISRO) launched *Astrosat* [1] on September 28, 2015. It was India's first dedicated multi-wavelength astronomy satellite and included 5 payloads: the Soft X-Ray imaging Telescope (SXT); the Large Area X-Ray Proportional Counters (LAXPC); the Cadmium Zinc- Telluride Imager (CZTI); the Scanning Sky Monitor (SSM); and the Ultra Violet Imaging Telescope (UVIT), the only ultraviolet (UV) telescope onboard.

There are two telescopes on the UVIT payload which simultaneously image the sky in the far ultraviolet (FUV: 1300-1800 Å) in one telescope, and the near ultraviolet (NUV: 2000 - 3000 Å) and visible (VIS: 3200-5300 Å) in the second telescope, with the bands separated using a dichroic mirror. The field of view (FOV) is  $\sim 28'$  diameter with a spatial resolution of  $\sim 1.4''$ . Specific bands are selected through a filter wheel on each telescope. The VIS data were intended to be used only for astrometric correction and have no scientific utility. The instrument has been described in Kumar et al[2].

An important product of a wide-field imaging mission is a point source catalog that may be correlated with catalogs in other wavelengths to yield a multi-wavelength picture of the sky. While numerous catalogs exist in the optical (e.g., *Sloan Digital Sky Survey* (SDSS) and *Panoramic Survey Telescope and Rapid Response System* (Pan-STARRS)) and infrared (e.g., *2-Mass Catalog*), fewer options are available in the UV due to the need for space-based observations. An early attempt was the TD-1 catalog [3] from the TD-1 mission, a satellite operated by the *European Space Research Organisation* (ESRO). The Ultraviolet Sky Survey Telescope onboard TD1 measured the absolute ultraviolet flux distribution of point sources between 1350Å- 2550Å, containing about 31,215 stars with a visual magnitude limit of  $\sim 10$  for unreddened early B type stars in its six-month observation period. The deepest UV catalog to date is from the *Galaxy Evolution Explorer* (GALEX) [4, 5], which was observed in two main bands (1350Å-1750Å and 1750Å-2750Å). The GALEX catalog includes data from three surveys: All-sky Imaging Survey (AIS), Medium Imaging Survey (MIS), and Deep Imaging Survey (DIS), covering approximately 25,000 sq. degrees of sky in its final data release. The AIS

provides a magnitude limit of  $\sim 20$ , while the MIS and DIS can detect sources up to magnitude limits of  $\sim 23$  and  $\sim 25$ , respectively.

There exist catalogs of small portions of the sky observed by UVIT. [6]Leahy et al. observed about 18 regions of the M31, and generated a catalog of  $\sim 75,000$  sources with a limiting magnitude of  $\sim 23$  in FUV CaF2-1 filter. [7]Devaraj et al. created a point source catalog from the observation of 3 overlapping fields in the outskirts of the SMC by the UVIT. The total number of sources detected was  $\sim 11,241$ . The catalog provided information about their AB magnitude in 7 UVIT filters, of which 3 are in the FUV and 4 in the NUV. In our work, we cover a larger area of the sky with a higher number of field images, including a few fields of SMC.

UVIT has completed about  $\sim 1700$  observations (including multiple observations of a single field) after almost 9 years of observations and we believe that it is time to construct a point source catalog ('*UVIT-cat*'). We begin with a sample of **428 fields** in the FUV and **54 fields** in the NUV covering about  $\sim 63$  square degrees of the sky and plan to expand the catalog to the entire UVIT data set. In Section 2, we explain the details of the UVIT instrumentation and data collection; in Section 3, we discuss the analysis and results; and in Section 4, we give a summary of our catalog and future work.

## 2 UVIT Instrument and Data

The Ultra Violet Imaging Telescope (UVIT) observed the sky in two UV and one visible band using two 38 cm telescopes. One telescope observed the far ultraviolet (FUV: 1300-1800 Å) while the other split the light into the near ultraviolet (NUV: 2000 - 3000 Å) and visible (VIS: 3200-5300 Å) bands. There are three identical intensified microchannel plates with an aperture of 40mm, and only the photocathode differs as given in Kumar et al [2]. A filter wheel on each telescope divided the spectral region into several bands (Table 1). The UVIT image pixel size is  $\simeq 0.4168''$  by  $0.4168''$ . The two UV detectors were operated in photon counting mode while the VIS channel was used only for attitude correction and was operated in integration mode.

UVIT data are processed and archived at the Indian Space Science Data Centre [8] and may be downloaded from the *Astrobrowse Archive*<sup>1</sup> in the following formats:

1. **Level 0:** The Level 0 is the raw binary data as observed by the UVIT payload onboard the *AstroSat*, along with its auxiliary data. This is sent to the AstroSat Data Centre at *Indian Space Science Data Centre* (ISSDC) for further processing into Level 1 data.
2. **Level 1:** The Level 1 data from the ISSDC is sent to the *Payload Operation Centre* (POC) at the Indian Institute of Astrophysics (IIA), Bengaluru. The files in the Level 1 data are FITS binary table files organized according to the orbit number under a single top-level directory as described in Rahna et al.[9].
3. **Level 2:** These are the final products after processing the Level 1 data through the UVIT pipeline software. The final product is a FITS image file, containing the coordinate information and can be read by any common astronomical data processing program.

As of 1st June 2024, there were a total of 1713 observations in the UVIT archive in both channels. The NUV channel ceased operation in March 2018, and only FUV data were taken since then. We have only used observations with an exposure time greater than 200 seconds. These are distributed in the sky as shown in Fig 1 and exclude the Galactic Plane, where there were no observations due to concerns about the sky brightness. The blue dots represent the images observed only through the FUV filter, while the green dots represent sources observed only through the NUV filter. We represent the pointings as red dots for field images observed through both FUV and NUV.

### 2.1 Astrometric Correction and Source Extraction

The astrometry in the Level 2 archival data file is off by several arcminutes, and each field has to be corrected individually. We first ran each image through *Astrometry.net* by Lang et al.[10], which used a set of stars (or galaxies) from a reference catalog (typically optical catalogs such as Tycho-2 and 2MASS) to solve for the astrometry in that image. This worked well for the NUV, where the sky looks similar to the optical, but the FUV sky is quite different from the visible sky, and we had to create a custom catalog based on GALEX FUV observations. There were still a few problematic fields, generally because there were too few stars in the field, which we corrected by matching stars by eye. The FITS files of the image headers having the updated World Coordinate system are in the GitHub repository<sup>2</sup>.

We used SExtractor v2.25.0 [11] to extract point sources from the astrometrically-corrected FITS files. We used the default parameters for extraction except as listed below:

<sup>1</sup>[https://astrobrowse.issdc.gov.in/astro\\_archive/archive/Home.jsp](https://astrobrowse.issdc.gov.in/astro_archive/archive/Home.jsp)

<sup>2</sup><https://github.com/swagatastro98/UVIT-cat.git>

Filter	Filtername	Mean $\lambda$ ( $\text{\AA}$ )	Zeropoint (ZP) (ZP)	passband (nm)
F148W	CaF2-1	1481	18.097	125–179
F154W	BaF2	1541	17.771	133–183
F169M	Sapphire	1608	17.410	145–181
F172M	Silica	1717	16.274	160–179
N242W	Silica-1	2418	19.763	194–304
N219M	NUVB15	2196	16.654	190–240
N245M	NUVB13	2447	18.452	220–265
N263M	NUVB4	2632	18.146	220–265
N279N	NUVN2	2792	16.416	273–288

Table 1: Filter details used for observations

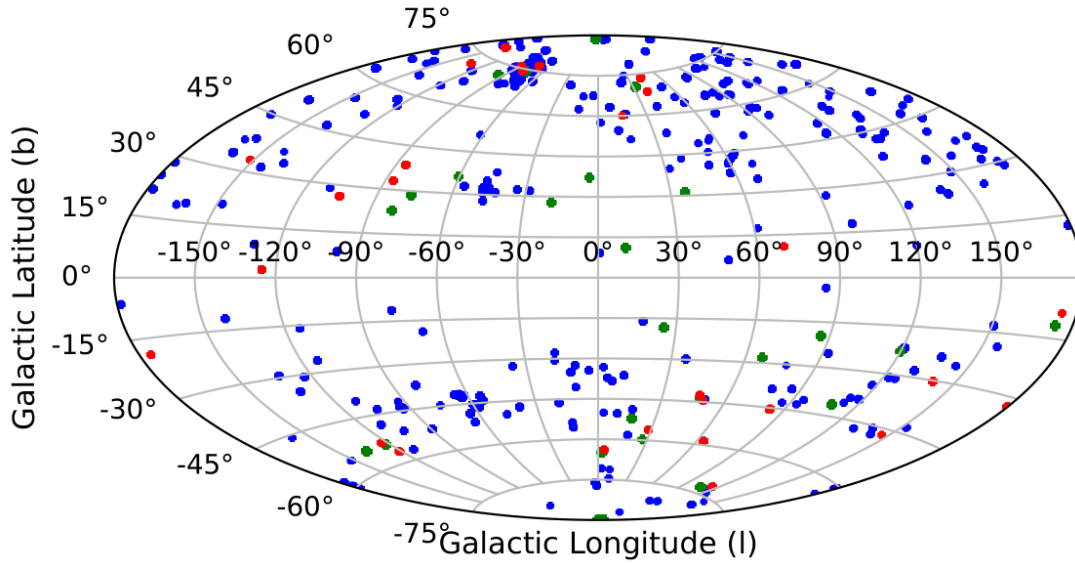


Figure 1: Area of sky covered by UVIT-cat. Blue: FUV fields only, Green: NUV fields only, and Red: Field images containing both FUV and NUV

Parameters	Values
DETECT_MINAREA	5
DETECT_THRESH (FUV/NUV)	3/5
ANALYSIS_THRESH	3
FILTER	default.conv
DEBLEND_NTHRESH	32
DEBLEND_MINCONT	0.005
PIXEL_SCALE	0.41657
BACK_TYPE	AUTO
BACK_SIZE	8 - 256
BACK_FILTERSIZE	1 - 3
CLEAN	Y
CLEAN_PARAM	0.1

Table 2: Source-Extractor default parameters

1. We changed DETECT\_MINAREA (the minimum number of adjacent pixels that have to be above a certain value for a detection) to 5 from 3 as per the PSF of the instrument.
2. The value for DETECT\_THRESH was set to be 3 for the FUV and 5 for NUV images to minimize the number of false detections. Setting a smaller threshold value (e.g. 1.5 times background) increased the false detection counts of higher exposure images. Hence, we chose an optimal value for the detection threshold such that there is minimum detection of false positives across the entire dataset.
3. We used the pixel scale of UVIT (0.4168'') for PIXEL\_SCALE
4. The zero point magnitude (MAG\_ZEROPOINT) of the instrument was varied for each filter, as per [12].

The detailed parameters used for source extraction are listed in Table 2

The source-extractor calculates the error in magnitudes by considering the error in the flux, which is given as:

$$\sigma_F = \sqrt{\sigma_{photon}^2 + \sigma_{sky}^2 + \sigma_{read}^2} \quad (1)$$

where,  $\sigma_{photon}$  is the photon noise,  $\sigma_{sky}$  is the background noise and  $\sigma_{read}$  is the readout noise associated with the detector.

The photon noise can be represented as the square root of flux in photon counts (F) from the source as:

$$\sigma_F = \sqrt{F} \quad (2)$$

The magnitude error,  $\Delta m$ , is calculated using the flux error value from equation (1) as:

$$\Delta m = \frac{2.5}{\ln 10} \left( \frac{\sigma_F}{F} \right) \quad (3)$$

The detection threshold parameters and the error calculation algorithm can be found in the manual at Source-extractor official website<sup>3</sup>.

## 2.2 Merging of duplicate sources

We combined the point source list from each observation into a single catalog. Any detection within 1.5'' of another was merged into a single source. A single binary FITS binary table is created from all observations of a single field, regardless of detector or filter. If multiple detections of the same source were present in the same filter, we took the mean of the magnitudes and flux. If multiple detections of a source were present in different filters, all the information is condensed into a single row in the FITS table. The number of sources having entries in FUV and NUV are given in Table 3 and 4.

<sup>3</sup><https://www.astromatic.net/software/sextractor/>

Filter-slot	Filter	Filter-name	Number of fields	Number of sources
F1	F148W	CaF2-1	190	44,289
F2	F154W	BaF2	157	16,161
F3	F169M	Sapphire	60	6,739
F5	F172M	Silica	17	2,690
F7	F148Wa	CaF2-2	4	1,574
Total			428	71,453

Table 3: Total number of sources through FUV filter

Filter-slot	Filter	Filter-name	Number of fields	Number of sources
N1	N242W	Silica-1	26	24,562
N2	N219M	NUVB15	7	546
N3	N245M	NUVB13	15	9,965
N5	N263M	NUVB4	3	1,942
N6	N279N	NUVN2	3	3,238
Total			54	40,253

Table 4: Total number of sources through NUV filter

### 3 Result and Analysis

#### 3.1 Image to Catalog Script

We have modified *jude\_call\_astrometry* procedure of JUDE (Jayant’s UVIT Data Explorer) [13, 9] to process the Level 2 UVIT images, correct the astrometry, and output a FITS binary table catalog file for each image. The columns are listed in Table 5. We then merged all the field catalogs into a single file (UVIT-cat). We have included all instances of different observations of the same field.

The UVIT catalog without any merging had about  $\simeq 117,598$  sources, of which 14,825 were duplicates. We merged the duplicate rows to come up with the UVIT-cat catalog that contains **102,773** NUV and FUV sources, observed through different filters of UVIT.

The matching algorithm merges all sources within a  $1.5''$  radius to give us a final merged catalog. The algorithm finds all sources within the radius by flagging them as duplicates, extracts the magnitudes, fluxes, and their errors from each row in a single filter, and computes the average, which is taken as the final photometry, and merged into a single row. If duplicate sources are found in separate filters, all the rows are merged into a single row with photometric entries in separate columns.

Many field images with extended sources like galaxies, nebulas, and densely crowded fields, are not yet included, and we intend to put forward updated versions of the catalog by including more UVIT field images, both in FUV and NUV.

#### 3.2 Completeness and Analysis of the Catalog

The number of fields along with their respective number of sources observed through each FUV and NUV filter of UVIT is given in Table 3 and 4 respectively. We find the highest number of observations and detections in the first filter of both NUV and FUV channels. 44,289 sources were found in the F148W filter (CaF2-1; F1) of FUV channel out of the 190 observations. A similar (157) number of observations were made through the filter F154W (BaF2; F2), but significantly less number of detections were made (16,161) as shown in Table 3. The number of sources detected is about  $\simeq 24,562$  as detected in the 26 fields of the NUV N242W filter. The next set of filters (N219M, N245M, N263M, and N279N) detected about 546, 9,965, 1,942, and 3,238 sources respectively. We found that the highest exposure time images were mostly observed through the F1 filter of FUV and NUV compared to the other filters, and this accounts for the highest number of detections of the first filter in each channel.

Tags	Columns
RA	Right ascension of the centroid position of the source
DEC	Declination of the centroid position of the source
N1_M_A	NUV Kron-like elliptical aperture magnitude (F1 filter)
N1_MER_A	NUV RMS error for elliptical aperture magnitude (F1 filter)
N1_M_I	NUV Isophotal magnitude (F1 filter)
N1_MER_I	NUV RMS error for isophotal magnitude (F1 filter)
FLAGS	Extraction flags
N1_F_A	NUV Flux within a kron-like elliptical aperture (F1 filter)
N1_FER_A	NUV Flux error within a kron-like elliptical aperture (F1 filter)
A_IMAGE	Profile RMS along major axis
B_IMAGE	Profile RMS along minor axis
A_WORLD	Profile RMS along the major axis (world units)
B_WORLD	Profile RMS along the minor axis (world units)
X_IMAGE	Object position along X-axis (in pixels)
Y_IMAGE	Object position along Y-axis (in pixels)
X_WORLD	Object position along X-axis (in degrees)
Y_WORLD	Object position along Y-axis (in degrees)
ERRA_IMG	RMS position error along major axis
ERRB_IMG	RMS position error along minor axis
ERRA_WLD	World RMS position error along major axis
ERRB_WLD	World RMS position error along minor axis
XY_WORLD	Covariance between X-world and Y-world
FWHM_WLD	FWHM of the object assuming a Gaussian core (in degrees)
FWHM_IMG	FWHM of the object assuming a Gaussian core (in pixels)
CLS_STR	Star/Galaxy classifier
ELLIP	Ellipticity; $1 - B\_image/A\_image$
THEJ2000	Position angle (J2000)
KRON_RAD	Kron apertures in units of A or B
GAL_RA	Galactic right ascension
GAL_DEC	Galactic declination
DIST_FOV	Distance of the object from the center of FOV
F1_M_A	FUV Kron-like elliptical aperture magnitude (F1 filter)
F1_MER_A	FUV RMS error for elliptical aperture magnitude (F1 filter)
F1_M_I	FUV Isophotal magnitude (F1 filter)
F1_MER_I	FUV RMS error for isophotal magnitude (F1 filter)
F1_F_A	FUV Flux within a kron-like elliptical aperture (F1 filter)
F1_FER_A	FUV Flux error within a kron-like elliptical aperture (F1 filter)

Table 5: UVIT-cat catalog summary

Bins/Filter-slot	Filter-F1	Filter-F2	Filter-F3	Filter-F5	Filter-F7
Bin1	20.527	20.568	20.065	19.523	21.474
Bin2	20.818	21.967	21.499	21.093	20.49
Bin3	21.98	22.907	22.032	20.614	No data

Table 6: Peak AB magnitude of source-count distribution of each filter of FUV

Bins/Filter-slot	Filter-F1	Filter-F2	Filter-F3	Filter-F5	Filter-F7
Bin1	21.283	21.033	20.587	19.97	21.561
Bin2	21.945	22.681	22.499	21.939	22.295
Bin3	23.671	23.769	22.822	22.356	No data

Table 7: Magnitude limit of all the filters of FUV in three bins

The images that were analyzed had a large variation of exposure time (from  $\sim 400$ s to more than 45,000s), influencing the catalog's completeness. To facilitate statistical studies, we divided the images into three bins based on exposure times. The first bin contained images with 2,000s or less exposure timing. The second bin ranged from 2,000 to 10,000s, and any image with exposure time greater than 10,000s was put into the third bin. The bins contained 246, 142, and 40 FUV images respectively. As shown in Fig 2, the magnitude limit will correspond to the median value of each of the three bins. For the first bin, we find the typical exposure of FUV images to be  $\sim 1798$ s. The second and third bins had the median exposure time at  $\sim 2,500$ s and  $\sim 11,000$ s respectively. The bins are separated with two vertical lines, green and red at the 2000s and 10,000s respectively. The histogram of the exposure time of NUV images is shown in Fig 4a, and we find out the median value to be  $\sim 400$ s.

The distribution of the AB magnitude of the detected sources in each of the 3 bins of the FUV channel and NUV channel is shown in Fig 3 and Fig 4b. The plots are shown for images observed via different filters of the FUV and NUV channels of UVIT.

We find the peak of the source count distribution as 20.527, 20.81, and 21.98 for the F1 filter in the three respective bins of exposure times as shown in Fig 3a, 3b and 3c. The peak magnitude distribution for the remaining filters of UVIT in FUV is tabulated in Table 6.

To compute the completeness of the catalog from the source count distribution in Fig 3 and Fig 4b, we find the turnover point where the number count of the sources falls drastically. The results are given in Table 7. We see that the completeness increases in Bin3, i.e. with higher exposure time.

In the NUV band, the N242W band with the highest number of detections has the turnover point around the magnitude  $\sim 22.602$ .

To determine the completeness from the magnitude vs magnitude error plot, we find the  $5\text{-}\sigma$  detection limit of the catalog's data. This corresponds to an error cut of 0.198; i.e. the faintest source which has a magnitude error of 0.198 or lower. The variation of magnitude error as a function of brightness (in AB magnitude) in the three bins is shown in Fig 5. For the F148W filter, the plot generated from each of the three bins shows the completeness at  $\sim 23.98$ , 24.30, and 24.91 respectively as shown in Fig 5a, 5c and 5e. For the second filter, we find the  $5\text{-}\sigma$  point at  $\sim 23.35$ , 23.80, and 25.12 in all the three bins, as given in Fig 5b, 5d and 5f. We find the limiting magnitude for the NUV N242W filter at about  $\sim 23.027$  (Fig 6a).

As we have combined all the observations into a single catalog, we found that around  $\sim 1800$ s exposure time, the highest number of observations has been made by UVIT. Hence, we can consider the magnitude limit of **Bin 1** as the completeness of the entire '*UVIT-cat*' catalog, i.e. for FUV, we get the magnitude limit to be around  $\sim 21$ , while for NUV, we find the completeness at around  $\sim 23$ .

We cross-matched the positions of our own UVIT catalog using the GALEX GUVcat and Gaia EDR3 catalog. For the following analysis, we plot and visualize the histogram distribution of angular separation of matched sources between the UVIT-cat catalog ( $\alpha, \delta$ ) and the reference catalog position ( $\alpha, \delta$ ) values respectively. We keep the separation threshold as  $5''$  and find all matches, i.e. we consider the source as a match if it falls within this radius. This is shown in Fig 7.

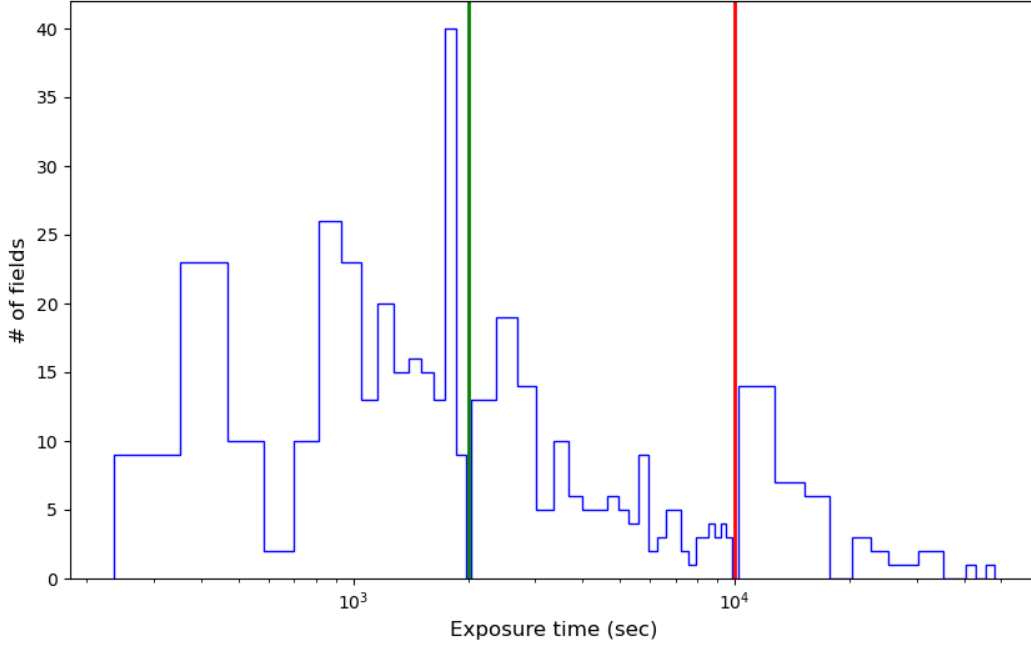


Figure 2: Exposure time histogram of 3 bins in FUV band, separated by (a)green: 2,000s and (b)red: 10,000s

We found the angular separation cross-matched with Gaia EDR3 to be  $\simeq 0.240''$ , as given in Fig 7a. Similarly, we found the average angular separation when compared with GALEX’s GUVcat to be  $\simeq 0.602''$ , as given in Fig 7b. This shows that our positions of the detected sources are in good agreement astrometrically with the already existing catalogs.

## 4 Conclusion and Future Work

In our work, we have analysed 428 FUV and 54 NUV UVIT field pointings and present *UVIT-cat* catalog. The UVIT-cat covers a total of  $\sim 63$  square degrees. We have come up with a catalog of  $\simeq 102,773$  sources in the 5 far ultraviolet and the near ultraviolet bands. The number of entries in each filter is tabulated in Table 3 and 4. The magnitude limit after statistical analysis is found to be,  $\sim 21.28, 21.03, 20.59, 19.523,$  and  $21.474$  for all FUV band filters respectively. The catalog contains 85 columns of data, and the description of the column keys is given in Table 5. The catalog will help the scientific community study objects such as QSOs, white dwarfs, young galaxies, and various astrophysical sources and provide a clear picture of the sky in the ultraviolet band.

### 4.1 Acknowledgement

This publication uses the data from *Indian Space Research Organisation’s (ISRO) AstroSat* mission. The data was available at the organization’s archive *Indian Space Science Data Centre(ISSDC)*, where the data was processed at the Payload Operation Center (POC) at the *Indian Institute of Astrophysics (IIA)*. The UVIT mission is accomplished in collaboration between IIA, *Inter-University Center for Astronomy and Astrophysics (IUCAA)*, *Tata Institute of Fundamental Research (TIFR)*, ISRO and *Canadian Space Agency (CSA)*. The authors would like to thank the anonymous reviewers for their insightful reviews and comments.

*Softwares:* IRAF [14], Astropy[15], Numpy[16], Pandas[17], Matplotlib[18], DS9, JUDE[13, 9], Astrometry.net [10].

*Data Availability:* The complete electronic version of the UVIT-cat catalog in FITS format and the header files containing the WCS information can be found in the GitHub repository <sup>4</sup>.

<sup>4</sup><https://github.com/swagatastro98/UVIT-cat.git>



## References

- [1] P. C. Agrawal. A broad spectral band Indian Astronomy satellite ‘Astrosat’. *Advances in Space Research*, 38(12):2989–2994, January 2006.
- [2] Amit Kumar, SK Ghosh, J Hutchings, PU Kamath, S Kathiravan, PK Mahesh, J Murthy, S Nagbhushana, AK Pati, MN Rao, et al. Ultraviolet imaging telescope (uvit) on astrosat. In *Space Telescopes and Instrumentation 2012: Ultraviolet to Gamma Ray*, volume 8443, pages 455–466. SPIE, 2012.
- [3] A. Boksenberg, R. G. Evans, R. G. Fowler, I. S. K. Gardner, L. Houziaux, C. M. Humphries, C. Jamar, D. Macau, D. Malaise, A. Monfils, K. Nandy, G. I. Thompson, R. Wilson, and H. Wroe. The Ultra-violet Sky-Survey Telescope in the TD-1A Satellite. *Monthly Notices of the Royal Astronomical Society*, 163(3):291–322, 08 1973.
- [4] D Christopher Martin, James Fanson, David Schiminovich, Patrick Morrissey, Peter G Friedman, Tom A Barlow, Tim Conrow, Robert Grange, Patrick N Jelinsky, Bruno Milliard, et al. The galaxy evolution explorer: a space ultraviolet survey mission. *The Astrophysical Journal*, 619(1):L1, 2005.
- [5] Luciana Bianchi, Bernie Shiao, and David Thilker. Revised catalog of galex ultraviolet sources. i. the all-sky survey: Guvcat\_ais. *The Astrophysical Journal Supplement Series*, 230(2):24, 2017.
- [6] DA Leahy, J Postma, Y Chen, and M Buick. Astrosat uvit survey of m31: point-source catalog. *The Astrophysical Journal Supplement Series*, 247(2):47, 2020.
- [7] Ashish Devaraj, Prajwel Joseph, CS Stalin, Shyam N Tandon, and Swarna K Ghosh. Uvit observations of the small magellanic cloud: Point-source catalog. *The Astrophysical Journal*, 946(2):65, 2023.
- [8] Kulinder Pal Singh, SN Tandon, PC Agrawal, HM Antia, RK Manchanda, JS Yadav, S Seetha, MC Ramadevi, AR Rao, D Bhattacharya, et al. Astrosat mission. In *Space Telescopes and Instrumentation 2014: Ultraviolet to Gamma Ray*, volume 9144, pages 517–531. SPIE, 2014.
- [9] P. T. Rahna, Jayant Murthy, and Margarita Safonova. JUDE (Jayant’s UVIT Data Explorer) pipeline user manual. *Journal of Astrophysics and Astronomy*, 42(2):35, October 2021.
- [10] Dustin Lang, David W. Hogg, Keir Mierle, Michael R. Blanton, and Sam T. Roweis. Astrometry.net: Blind astrometric calibration of arbitrary astronomical images. *The Astronomical Journal*, 139:1782 – 1800, 2009.
- [11] Emmanuel Bertin and Stephane Arnouts. SExtractor: Software for source extraction. *Astronomy and astrophysics supplement series*, 117(2):393–404, 1996.
- [12] SN Tandon, J Postma, P Joseph, A Devaraj, A Subramaniam, IV Barve, K George, SK Ghosh, V Girish, JB Hutchings, et al. Additional calibration of the ultraviolet imaging telescope on board astrosat. *The Astronomical Journal*, 159(4):158, 2020.
- [13] J. Murthy, P. T. Rahna, F. Sutaria, M. Safonova, S. B. Gudennavar, and S. G. Bubbly. JUDE: An Ultraviolet Imaging Telescope pipeline. *Astronomy and Computing*, 20:120–127, July 2017.
- [14] Doug Tody. The iraf data reduction and analysis system. In *Instrumentation in astronomy VI*, volume 627, pages 733–748. SPIE, 1986.
- [15] Adrian M Price-Whelan, Pey Lian Lim, Nicholas Earl, Nathaniel Starkman, Larry Bradley, David L Shupe, Aarya A Patil, Lia Corrales, CE Brasseur, Maximilian Nöthe, et al. The astropy project: sustaining and growing a community-oriented open-source project and the latest major release (v5. 0) of the core package. *The Astrophysical Journal*, 935(2):167, 2022.
- [16] Charles R Harris, K Jarrod Millman, Stéfan J Van Der Walt, Ralf Gommers, Pauli Virtanen, David Cournapeau, Eric Wieser, Julian Taylor, Sebastian Berg, Nathaniel J Smith, et al. Array programming with numpy. *Nature*, 585(7825):357–362, 2020.
- [17] Wes McKinney et al. pandas: a foundational python library for data analysis and statistics. *Python for high performance and scientific computing*, 14(9):1–9, 2011.
- [18] John D Hunter. Matplotlib: A 2d graphics environment. *Computing in science & engineering*, 9(03):90–95, 2007.

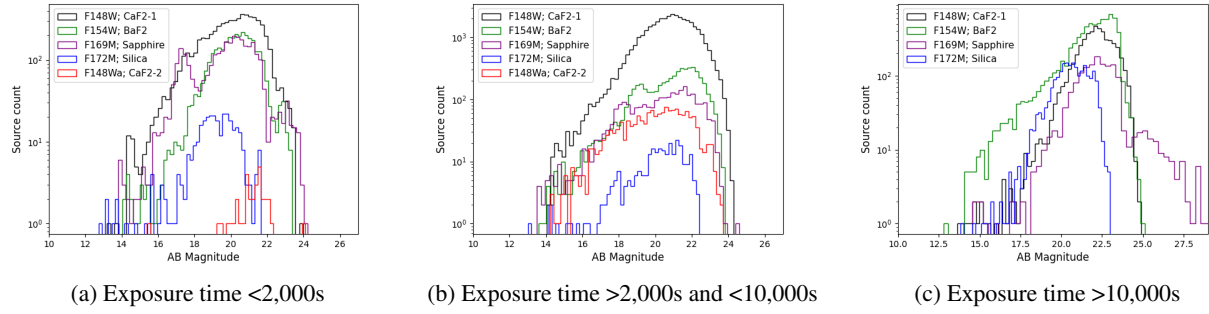


Figure 3: AB magnitude vs Source count distribution for 3 bins in FUV band

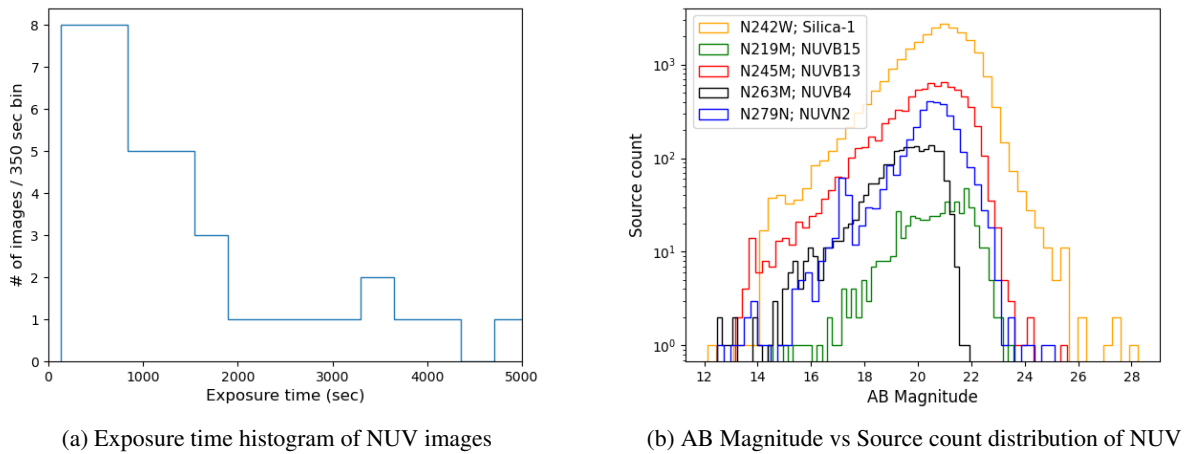


Figure 4: (a) Histogram of exposure times in NUV band (b) AB magnitude vs Source count distribution of NUV filters

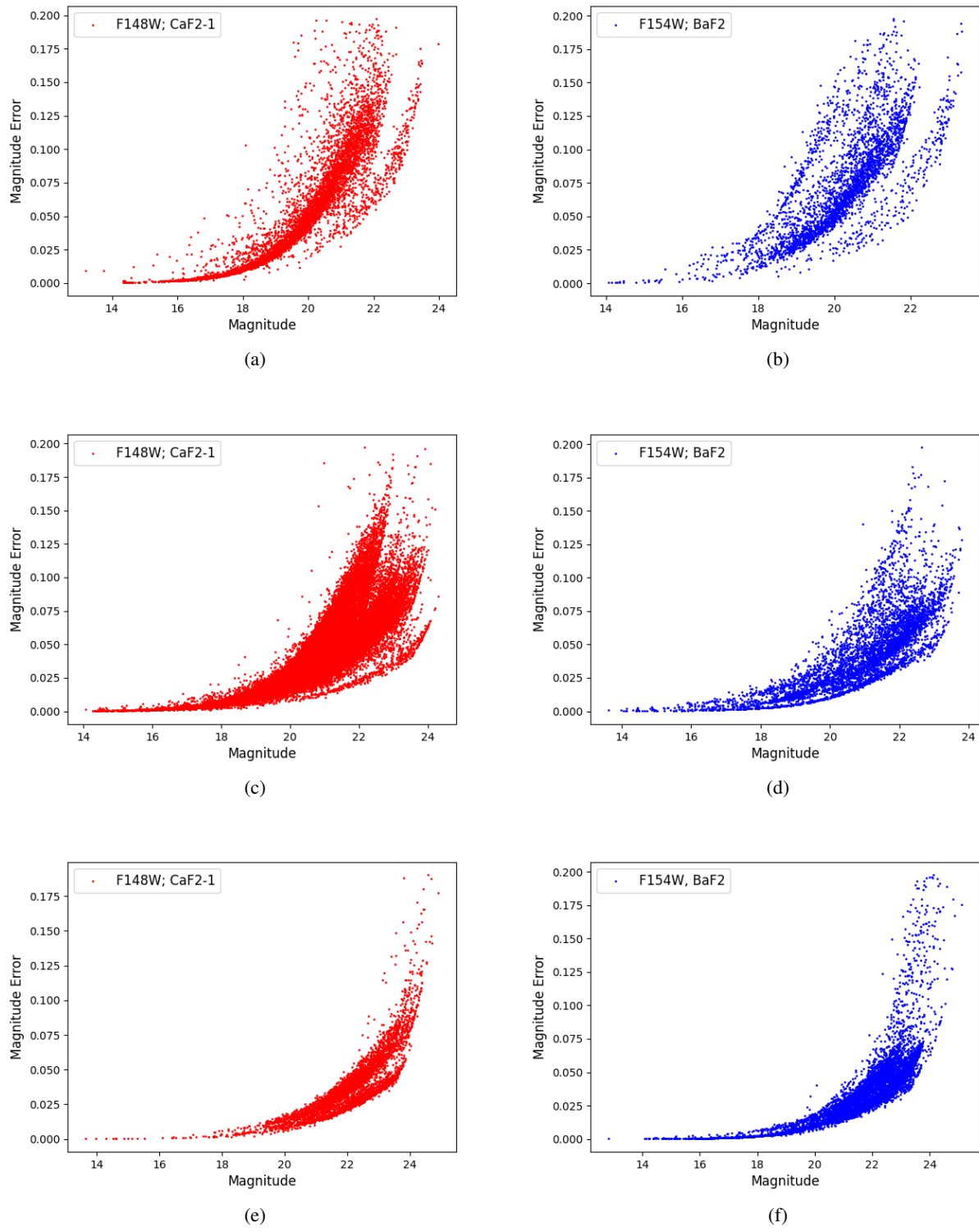


Figure 5: AB Magnitude vs AB Magnitude error for filters: FUV CaF2-1 (148W) and BaF2 (F154W) of UVIT. (a),(b): Bin 1, (c),(d): Bin 2 and (e),(f): Bin 3

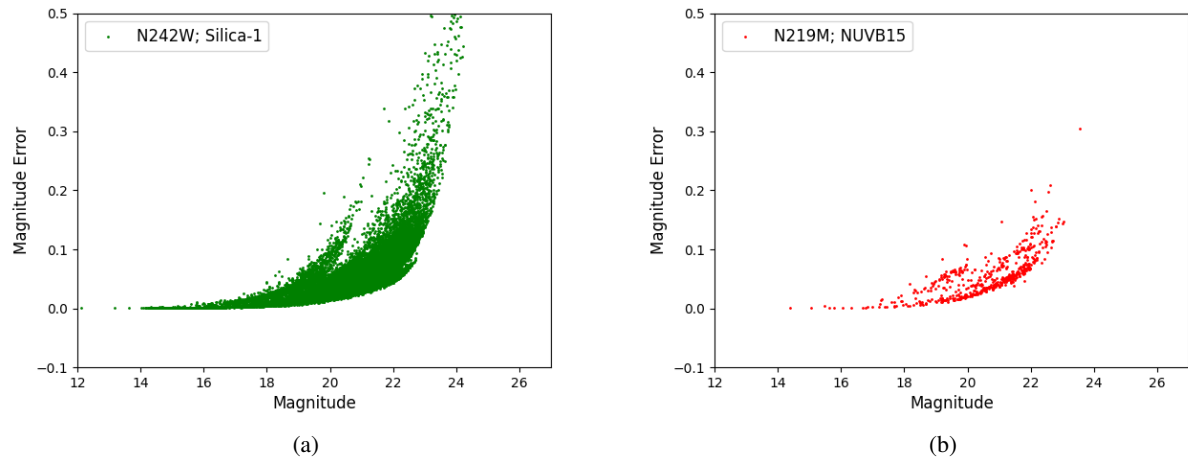


Figure 6: AB Magnitude vs AB Magnitude error for NUV filters: (a) NUV Silica-1 (N242W) and (b) NUVB15 (N219M) of UVIT

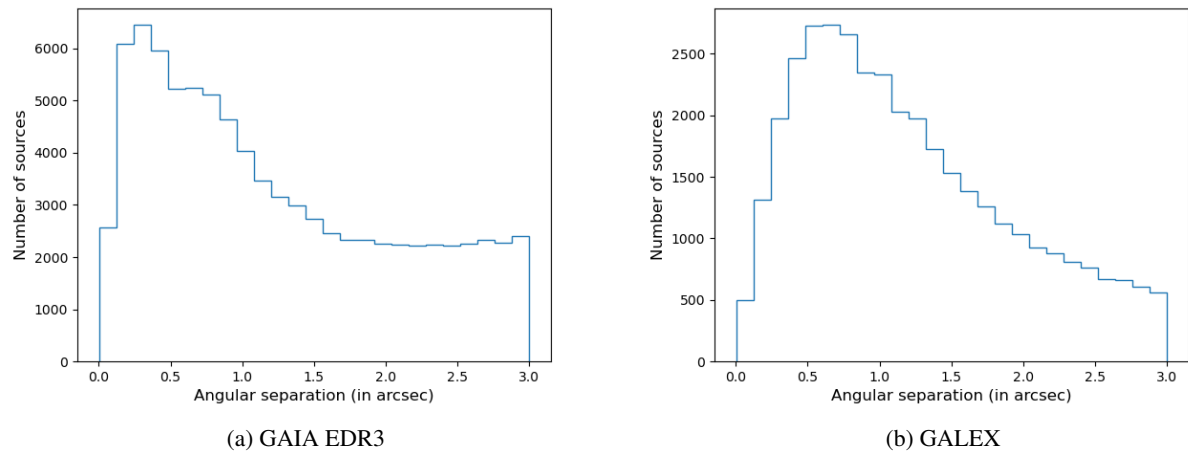


Figure 7: Angular separation distribution of UVIT with (a) GAIA EDR3 (b) GALEX